

January 2006

# Low-frequency noise statistics for the breakdown characterization of ultrathin gate oxides

N. Z. Butt

*School of Electrical and Computer Engineering, nbutt@purdue.edu*

A. M. Chang

*Department of Physics, Purdue University; Department of Physics, Duke University, changam@purdue.edu*

H. Raza

*Birck Nanotechnology Center and School of Electrical and Computer Engineering, Purdue University, hraza@purdue.edu*

Rashid Bashir

*Birck Nanotechnology Center and School of Electrical and Computer Engineering, Purdue University, bashir@purdue.edu*

J. Liu

*Electrical and Computer Engineering, University of Texas at Austin*

*See next page for additional authors*

Follow this and additional works at: <http://docs.lib.purdue.edu/nanopub>

---

Butt, N. Z.; Chang, A. M.; Raza, H.; Bashir, Rashid; Liu, J.; and Kwong, D. L., "Low-frequency noise statistics for the breakdown characterization of ultrathin gate oxides" (2006). *Birck and NCN Publications*. Paper 41.  
<http://docs.lib.purdue.edu/nanopub/41>

This document has been made available through Purdue e-Pubs, a service of the Purdue University Libraries. Please contact [epubs@purdue.edu](mailto:epubs@purdue.edu) for additional information.

---

**Authors**

N. Z. Butt, A. M. Chang, H. Raza, Rashid Bashir, J. Liu, and D. L. Kwong

## Low-frequency noise statistics for the breakdown characterization of ultrathin gate oxides

N. Z. Butt

*School of Electrical and Computer Engineering, Purdue University, West Lafayette, Indiana 47907*

A. M. Chang<sup>a)</sup>

*Department of Physics, Purdue University, West Lafayette, Indiana 47907-1396  
and Department of Physics, Duke University, Durham, North Carolina 27708-0305*

H. Raza and R. Bashir

*Birck Nanotechnology Center, Purdue University, West Lafayette, Indiana 47907  
and School of Electrical and Computer Engineering, Purdue University, West Lafayette, Indiana 47907*

J. Liu and D. L. Kwong

*Electrical and Computer Engineering, University of Texas at Austin, Austin, Texas 78712-0240*

(Received 9 August 2005; accepted 2 February 2006; published online 13 March 2006)

We have investigated the *statistics* of low-frequency noise in the tunneling current of ultrathin oxides (2.5–4 nm) in metal-oxide-semiconductor capacitors as a function of the applied voltage stress. The statistical analysis includes (i) non-Gaussianity (nG), which is a measure of the degree of temporal correlation in the noise, and (ii) ratio of integrated noise power to the dc leakage current ( $R$ ). The occurrence of high peaks in nG indicates the appearance of new percolation paths, and the subsequent conduction through these paths is indicated by  $R$ . Our results show that the nG and  $R$  characteristics are generic for the oxides of different thickness and growth quality and have the potential, in conjunction with leakage itself, of being used as a prognosticator of oxide reliability. © 2006 American Institute of Physics. [DOI: [10.1063/1.2186114](https://doi.org/10.1063/1.2186114)]

There has been a growing desire to precisely characterize the process of oxide breakdown to have an accurate estimation for the reliability of ultrathin gate oxides of metal-oxide-semiconductor transistors. When a voltage stress is applied across an ultrathin capacitor, the conduction through it can be categorized as of two types. One is the direct tunneling of carriers through the oxide barrier and the other is the tunneling through the defects (traps) present in the oxide, which is called the trap-assisted tunneling (TAT). With the increase of stress, the density of traps increases and new conduction paths are formed inside the oxide, giving rise to breakdown events. In thinner oxides the characterization becomes difficult because the breakdown events are often very soft, and are not easily detected in the (commonly measured) average leakage current density. On the contrary, it was earlier reported that the low frequency  $1/f$  noise in the tunneling current can be very sensitive to the damage associated with the trap assisted processes<sup>1–5</sup> and it was observed that the emergence of transient current spikes in TAT made the noise highly non-Gaussian. In our work, we have studied the characteristics of noise in SiO<sub>2</sub> capacitors by applying a ramp of voltage stress ( $V_g$ ) at the gate in small incremental steps: these capacitors have an area  $\sim 10^{-4}$  cm<sup>2</sup> and differ for the oxide thickness and the growth process. Analyzing the statistics of noise in each  $V_g$  step, we found interesting signatures in non-Gaussianity (nG) which is a measure of the degree of temporal correlation in the noise and the ratio of integrated noise power to the dc leakage current ( $R$ ), which are supposed to be closely related to the creation and development of percolation paths leading to hard and soft breakdowns (HBD and SBD, respectively). In contrast, no notable

features, in either nG or  $R$ , were observed in a 100 M $\Omega$  resistor or in any capacitor after it had undergone a HBD. These signatures of breakdown pathways were similar in oxides of different thickness and growth, although the magnitude of the stress needed to observe them was higher for good quality devices. The following three phenomena, which occurred sequentially, were involved in the breakdown (BD) pathway occurring at a certain  $V_g$ : (i) the appearance of nG peaks in the noise, (ii) the jumps in  $R$ , and (iii) an increase in the stress induced leakage current (SILC). The very first indication that a BD might occur was the presence of large peaks in nG, which were a result of the appearance of sharp transitory spikes in TAT. This was due to the creation of transitory conduction paths, in the oxide layer, from newly generated traps. The subsequent development of conduction through these transitory paths was manifested in the corresponding values of  $R$  as a function of  $V_g$ . In a breakdown pathway, peaks, due to the increased fluctuations (noise) in TAT, were observed in  $R$ —while there was no significant increase in the dc leakage current density  $J_{dc}$ : These fluctuations were presumably a direct consequence of conduction through the developing percolation paths through the oxide. Additionally it was found that a correlation existed between the magnitude and the spread (over  $V_g$ ) of the  $R$  peaks on one side and the damage in the device, detected by the increased values of SILC at the corresponding  $V_g$ , on the other.

In particular, the magnitude of an  $R$  peak correlated to the severity of BD and its spread over  $V_g$ , to the progressiveness of BD. Based on these metrics, we found three types of breakdown in devices according to their severity and progressiveness. Type I was those SBDs characterized by small narrow jumps in  $R$ . These were not progressive and had a mild impact on damage depicted in SILC. Type II was SBDs

<sup>a)</sup>Electronic mail: [yingshe@phy.duke.edu](mailto:yingshe@phy.duke.edu)

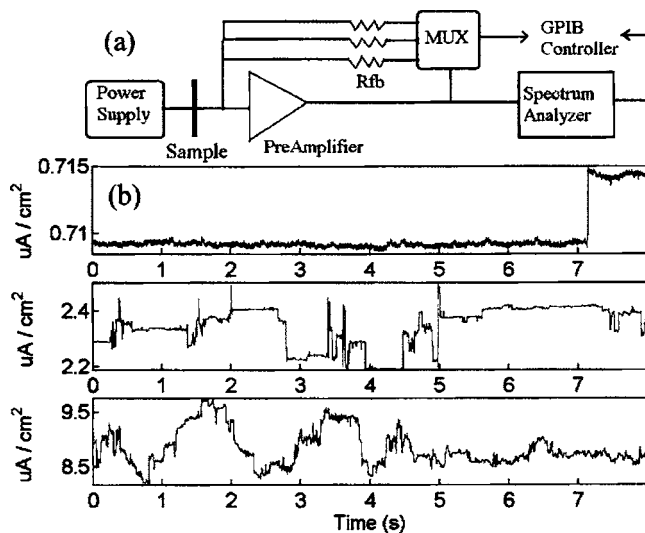


FIG. 1. (a) The experimental setup. (b)–(d) Examples of time traces of leakage current density ( $J_{dc}$ ) illustrating the sequence of a progressive BD in a 4 nm oxide. Traces (b)–(d) were measured at incremental  $V_g$  values in the range spread by a big  $R$  peak: (b) appearance of sharp current spike which resulted in high nG in noise before any increase in  $R$ , (c) sharp increase in noise with a relatively small increase in  $J_{dc}$  which resulted in a big jump in  $R$ , and (d) increase in  $J_{dc}$  due to added SILC contribution from the BD with no further increase in noise; this resulted in the falling of an  $R$  peak.

which showed big peaks in  $R$  spread over a wide range of  $V_g$  indicating the progressive damage to the percolation path. This type of BD had a significant impact on SILC. Type III was HBDs which were indicated by narrow but very sharp increase in both  $R$  and SILC. These were rare in occurrence even in thicker oxides but were most severe to the oxide damage. The noise statistics based on nG and  $R$  can thus be a very useful probe of different types of BD events in oxides and can be used as a complement to the high sensitivity  $I$ - $V$  measurements in order to precisely predict the reliability of ultrathin oxides.

An example of time traces illustrating the sequence of a progressive (type II) breakdown is shown in Fig. 1. The sharp jump of a relatively low magnitude in  $J_{dc}$  in Fig. 1(b) is a type of transitional current spikes, which resulted in high nG in noise. Until this point, there was no indication of breakdown in  $R$  or in  $J_{dc}$ . Figure 1(c) shows the onslaught of spikes in TAT which indicated the start of a very noisy conduction presumably through a single percolating path. The increase of noise was large compared to the increase in  $J_{dc}$  which resulted in a big jump in  $R$ . The trace in Fig. 1(d) indicates conduction through the percolation path during the final stage of BD when noise stopped increasing and  $J_{dc}$  had a significant increase due to added SILC contribution from the BD.

We have measured different quality oxides, which differed for their thickness (in the range 2.5–4 nm) and their growth conditions. The 2.5 nm samples were fabricated by Texas Instruments. The 4 nm oxides were grown in Purdue by dry oxidation for 30 min at 750 °C at atmospheric pressure. The substrates were  $p$ -type silicon with boron doping of  $\sim 10^{15} \text{ cm}^{-3}$  and the gates were fabricated in aluminum deposited by electron-beam evaporation. The capacitors were patterned and etched with different areas ranging from  $78 \times 10^{-6} \text{ cm}^2$  to  $650 \times 10^{-6} \text{ cm}^2$ . The 3.35 nm samples were provided by Bell-Laboratories and were grown by rapid thermal annealing. The presence of a large density of native traps

in the oxide was already known in this growth.<sup>6</sup> The thickness was verified by ellipsometry and cross-section TEM. The experimental setup is shown in Fig. 1(a) and consisted of a variable power supply, a low noise preamplifier to measure the current and a Stanford Research Systems SR785 spectrum analyzer [Fig. 1(a)].

The noise characteristics were observed by applying a negative voltage stress at the gate in incremental steps of 0.2 V. At each of these  $V_g$  steps, about 300 traces (8 s each) of the gate leakage current were taken. The time traces were Fourier transformed after subtracting the dc current ( $I_{dc}$ ) and the average power spectral density thus calculated was then integrated through the total bandwidth to obtain the integrated power spectral density (PSDI). The background noise was found to be a combination of the current and voltage noise of the operational amplifier and was subtracted from the  $1/f$  noise. The sensitivity of the measurements was down to  $4 \text{ fA}/\sqrt{\text{Hz}}$  at 10 Hz.  $R$  was calculated by the ratio:  $R = \text{PSDI}/I_{dc}^2$ . The non-Gaussianity of noise was computed at each of the constant voltage step using the expression:<sup>1</sup>  $\text{nG} = \langle (S_i - S_{av})^2 \rangle n_b / S_{av}^2$ , where  $S_i$  is the average noise power in a single Fourier transform,  $S_{av}$  is the average noise power for a set of  $N$  measurements,  $n_b$  is the total number of bins in the bandwidth, and the brackets  $\langle \rangle$  denote averaging over the set of  $N$  measurements. This quantity, nG, is simply a normalized variance of a series of noise power measurements and is a statistical test very sensitive to the transients in the time traces.<sup>1</sup> For a  $1/f$  signal, without any transients, the noise was Gaussian with  $\text{nG} \sim 1$  as can be seen from the results for a 100 M $\Omega$  resistor in Fig. 2(a).

For each of the three types of devices, an example of nG and  $R$  vs  $V_g$  is shown in Figs. 2(a)–2(c) for the first run of voltage stress. The second derivative of  $\log(I_{dc})$  normalized by the  $|\log(I_{dc})|$  is also plotted ( $D2$ ): the jumps in  $D2$  represent the damage to the oxide showed up in the local increase of SILC. In Fig. 2, the vertical lines separate the regions of BDs of different types ( $A, B, C, \dots, M$ ). Large nG peaks started to appear in the 4 nm device shown in Fig. 2(a) from very low  $V_g$  and the small peaks in  $R$  illustrated type I breakdown (regions  $A$ – $D$ ). A type II breakdown initiated with a big jump in  $R$  around 4 V (region  $E$ ). The wide spread of  $R$  indicated a progressive damage, during which, SILC increased gradually as also indicated by a number of  $D2$  jumps. The 3.35 nm device in Fig. 2(b) showed a small peak in nG and  $R$  in region “ $G$ ” after which  $R$  became steady until a type II BD showed up around 2 V (region  $H$ ). It should be noted that due to a large density of native traps in 3.35 nm growth, this device had an excessive leakage density even at very low  $V_g$  [Fig. 2(b), inset (i)]. The averaging effect of large number of readily available paths might be the reason that no sharp jumps in nG were observed in this device. Rather a steady rise of nG was observed with increasing  $V_g$  which might be an indication that some particular transitory paths were gradually dominating over others. Finally, this device showed a type III BD illustrated by a big sharp  $R$  jump as well as a jump in the SILC at approximately 5 V [Fig. 2(b) and inset (i)]. The characteristics of 2.5 nm device which are shown in Fig. 2(c) illustrate type I breakdowns in a 2.5 nm oxide. The jumps in  $R$  and  $D2$  were smaller and no type II or type III breakdowns were observed. The relatively significant jumps were found in region “ $K$ ” which was followed by a number of small jumps in regions “ $L$ ” and “ $M$ .”

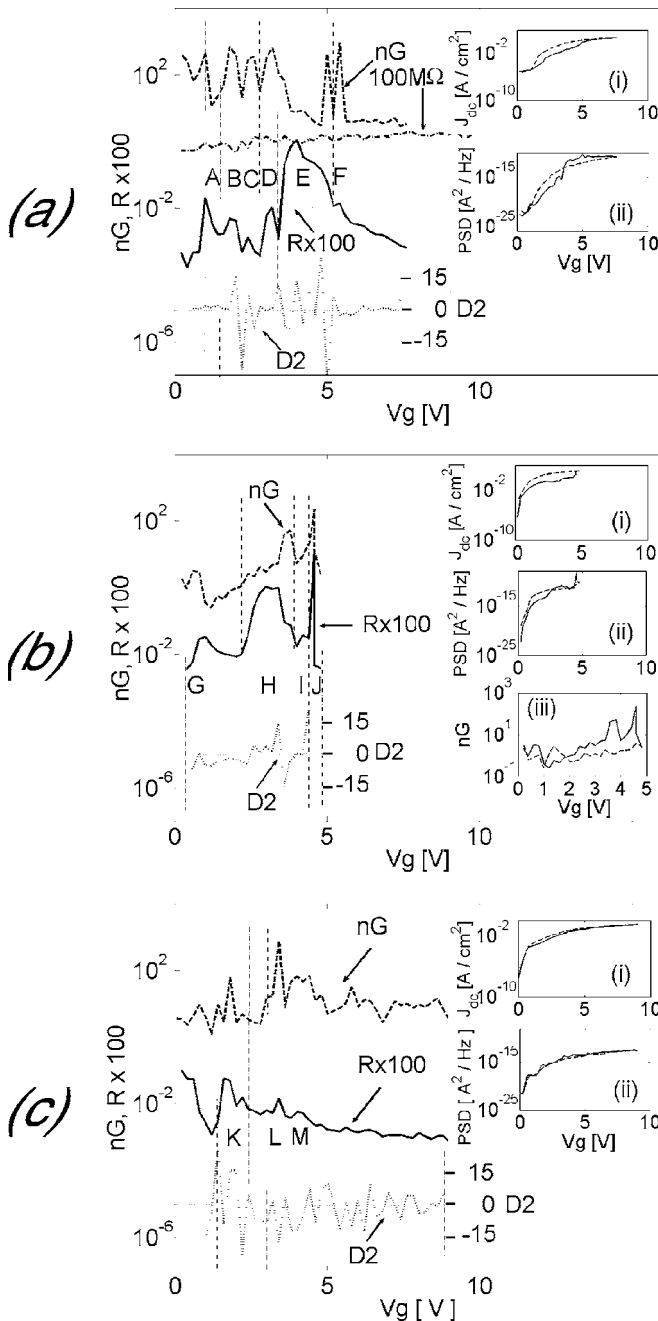


FIG. 2. The nG,  $R$ , and  $D2$  characteristics during the first run of voltage stress for (2a) 4 nm device, (2b) 3.35 nm device, and (2c) 2.5 nm device. The solid and the dashed styles represent  $R \times 100$  and nG, respectively, both as a function of  $V_g$ . The dash-dot curve in Fig. 2(a) is the nG characteristics of a 100 M $\Omega$  resistor measured by applying a run of  $V_g$  stress. The insets (i) and (ii) show  $J_{dc}$  vs  $V_g$  and PSD vs  $V_g$  characteristics respectively for two consecutive run of stress. The inset (iii) in Fig. 2(b) shows the nG in two consecutive runs of stress to the 3.35 nm device. The solid and the dashed styles represent the first and the second runs, respectively, in all the insets. The polarity of the voltage was negative at the gate for all data presented in this study. The vertical columns labeled as A, B, C, etc. indicate different regions of breakdowns during the  $V_g$  stress.

The absence of more severe BD types (I and II) could be due to either or both of the following reasons: (i) the presence of very few native traps due to a better good growth quality (ii) the lesser oxide thickness might had an effect to reduce the

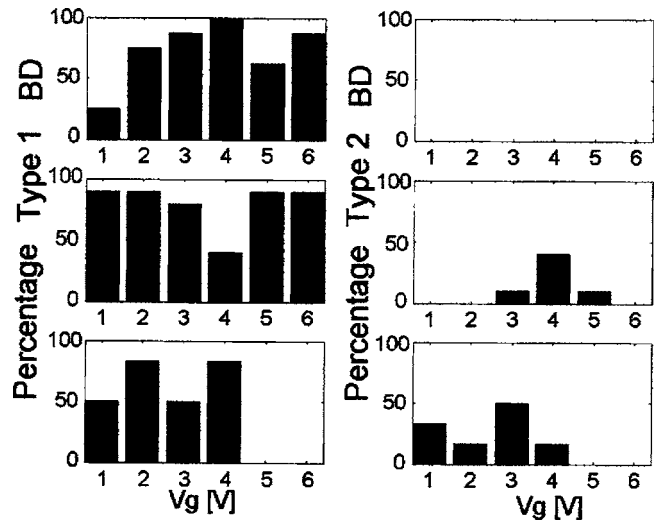


FIG. 3. The statistics of type 1 and type 2 BD occurrences at different magnitudes of the applied stress. The three rows from top to bottom show statistics of 3.35, 4, and 2.7 nm technologies, respectively. The numbers of devices tested in each technology were 6, 10, and 10, respectively.

probability of both progressive (type II) and hard (type III) BDs.

The statistics of type I and type II breakdowns, in three different oxide types, are shown in Fig. 3. Type III breakdown is not shown since it was observed not more than one of the 3.35 nm devices. These statistics represent the percentage breakdowns in the each of the three oxide types as a function of  $V_g$ . The probabilities for BD correlate well with the device quality, where the better quality devices show a reduced tendency for BD at a given stressing voltage.

Aside from the ability to distinguish between three types of qualitatively different BD processes, the most notable finding of our noise characterization is that while the pathway to BD qualitatively appears remarkably similar for oxides of differing quality, the noise signatures differ quantitatively. This bodes well of further development of the noise characterization method as a sensitive tool to ascertain oxide quality and to study the mechanism of BD, e.g., in order to distinguish between different models of SBD.<sup>7-9</sup>

The authors would like to acknowledge Tom Sorsch for providing the 3.35 nm Bell-Labs samples. This work was supported by NSF ECS 0100202.

<sup>1</sup>G. B. Alers, K. S. Krisch, D. Monroe, B. E. Weir, and A. M. Chang, Appl. Phys. Lett. **69**, 2885 (1996).  
<sup>2</sup>J. E. Sanchez, G. Bosman, and M. E. Law, IEEE Trans. Electron Devices **50**, 1353 (2003).  
<sup>3</sup>J. C. Ranuarez, M. J. Deen, and C. Chih-Hung, IEEE Electron Device Lett. **26**, 550 (2005).  
<sup>4</sup>C. L. F. Ma, M. J. Deen, and R. H. S. Hardy, Can. J. Phys. **70**, 1005 (1992).  
<sup>5</sup>G. B. Alers, B. E. Weir, M. A. Alam, G. L. Timp, and T. Sorch, Proc. IRPS **36**, 76 (1998).  
<sup>6</sup>A. Ghetti, E. Sangiorgi, T. W. Sorsch, and I. Kizilyalli, Microelectron. Eng. **48**, 31 (1999).  
<sup>7</sup>J. S. Suehle, B. Zhu, Y. Chen, and J. B. Bernstein, Microelectron. Reliab. **45**, 419 (2005).  
<sup>8</sup>M. A. Alam and R. K. Smith, Proc. IRPS, 406 (2003).  
<sup>9</sup>F. Monsieur, E. Vincent, D. Roy, S. Bruyere, G. Pananakakis, and G. Ghibaudo, Proc. IRPS, 45 (2002).